Original Article

3D-segmentation and characterization of visceral and abdominal subcutaneous adipose tissue on CT: influence of contrast medium and contrast phase

Robin F. Gohmann[1,2]^, Sebastian Gottschling[1], Patrick Seitz[1], Batuhan Temiz[2], Christian Krieghoff[1], Christian Lücke[1], Matthias Horn[3], Matthias Gutberlet[1,2]

[1]Department of Diagnostic and Interventional Radiology, Heart Center Leipzig, Leipzig, Germany; [2]Medical Faculty, University of Leipzig, Leipzig, Germany; [3]Institute for Medical Informatics, Statistics and Epidemiology (IMISE), University of Leipzig, Leipzig, Germany

Correspondence to: Robin F. Gohmann, MD. Department of Diagnostic and Interventional Radiology, Heart Center Leipzig, Strümpellstraße 39, 04289 Leipzig, Germany. Email: robin.gohmann@gmx.de.

Background: Adipose tissue as part of body composition analysis may serve as a powerful biomarker. Validation of segmented adipose tissue and correlation to clinical data has been performed on non-enhanced scans (NES). As many patients require a contrast enhanced scan (CES) for other aspects of clinical decision making, the utility of CES for body composition analysis would be most useful. Therefore, we analyzed the influence of iodinated contrast medium (ICM) and contrast phase on the characterization and segmentation of adipose tissue.

Methods: Exams of 31 patients undergoing multi-phasic CT at identical scan settings containing an NES were retrospectively included. In addition to NES, patients received an arterial (ART) (n=23), portal-venous (PVN) (n=10), and/or venous scan (VEN) (n=31) after intravenous injection of 90 mL ICM. Density and volume of adipose tissue were quantified semi-automatically with thresholds between –190 HU and –30 HU and recorded separately for visceral (VAT) and subcutaneous adipose tissue (SAT). Density and volume of total adipose tissue (TAT) were computed. For conversion of values from CES into those of NES regression analyses were performed and tested.

Results: Density of adipose tissue increased after application of ICM more on later scans (VEN ≈ PVN > ART) and more markedly in VAT than SAT (VAT > TAT > SAT). Except in SAT on ART, all changes were significant (P<0.001). Measured volume of adipose tissue decreased on all CES (VEN ≈ PVN > ART) (P<0.001), but only reached statistical significance for VAT and TAT (VAT > TAT) on all CES (P<0.05). Density and volume in CES correlate extremely well with NES and may be calculated from one another [root-mean-square error (RMSE): <6 HU; <0.85 dm^3].

Conclusions: Density and volume of segmented adipose tissue are altered by the injection of ICM in differing degrees between compartments and contrast phases. However, as the effect of ICM is fairly constant for a given compartment and contrast phase, values may be converted into those of NES with relative precession. This conversion allows body composition analysis to be carried out also in contrast enhanced CT examinations, e.g., for risk stratification and the comparison of the obtained results to previous studies.

Keywords: Body composition; segmentation; adipose tissue; contrast media; computed tomography

Submitted Jul 25, 2020. Accepted for publication Sep 22, 2020.
doi: 10.21037/qims-20-907
View this article at: http://dx.doi.org/10.21037/qims-20-907

^ ORCID: 0000-0001-8629-8490.

Introduction

Body composition analysis is a powerful tool for the assessment of frailty, metabolic characterization, cardiovascular risk stratification and risk assessment prior to major surgery or chemotherapy, potentially utilizing CT with adipose tissue being one of the key metrics for evaluation (1-6). CT was first proposed for body composition analysis in the early 1980s with Kvist *et al.* introducing systematically evaluated thresholds forming the basis for semi-automatic segmentation of adipose tissue (7). This technique ultimately proved to be much more precise and reproducible than previous methods such as nuclear medicine and anthropometric techniques or bioelectrical impedance analysis (8-12).

Validation of segmented adipose tissue and correlation to clinical data has been performed on non-enhanced scans (NES) (1,7,9-11,13). Only few studies have analyzed the effect of iodinated contrast medium (ICM) on quality and quantity of segmented adipose tissue (14-16). These studies have examined a limited range of contrast phases in only parts of the abdomen and have only rarely accounted for potentially confounding factors. However, the utility of contrast enhanced scans (CES) for body composition analysis with the possibility of comparing the obtained values to other studies would be most convenient as many patients require a CES for other aspects of clinical decision making. Some studies already utilize fat segmented from CES for risk assessment, but comparing these results to those of previous works would only be possible with severe limitations (17,18).

The aim of our study was to analyze the influence of contrast medium and contrast phase on the characterization and segmentation of adipose tissue in the visceral and subcutaneous abdominal compartment through three commonly acquired contrast phases in CT. A secondary goal was to assess whether or not one can convert values obtained from CES into those of NES by means of conversion formulae.

Methods

Study design

We retrospectively included 31 consecutive CT-studies of 31 patients with an NES and at least one CES of the abdomen after intravenous injection of 90 mL ICM (iohexol 350 mgI/mL, Accupaque 350, GE Healthcare, Munich, Germany) with identical scan parameters (Table S1), scanned with the same CT-scanner (Somatom Definition Flash, Siemens, Erlangen, Germany). ICM was applied via a catheter of 20 gauge or larger at the upper limb at an injection rate of 4.0 mL/s. No enteral contrast medium was applied. The inclusion criteria were constant parameters of scans within each examination, identical reconstruction of images and identical application of contrast medium. No further selection took place. In total 95 scans were included: 31 NES, 23 arterial (ART), 10 portal-venous (PVN) and 31 venous (VEN).

The study was conducted in compliance with the Declaration of Helsinki (Medical Association 2013). The local ethics committee approved the study (reference number: 337/19-ek) and written informed consent was waived.

CT acquisition

For ART a bolus-track technique was employed with the region of interest placed at the proximal abdominal aorta; the scan was initiated 5 s after reaching a threshold of 120 HU. PVN was initiated 20 s after ART. VEN was initiated either 90 s after injection of ICM, 50 s after ART or 30 s after PVN to achieve very similar delays after injection of ICM across individual exams.

Baseline characteristics and scan demographics

The leading clinical indications for CT were suspected vascular pathologies (e.g., bleeding), followed by oncological pathologies. Further baseline characteristics and scan demographics are shown in *Table 1*.

Image reconstruction and analysis

Images were reconstructed with a slice thickness and increment of 3 mm with a medium smooth filtered back projection kernel (B30f). For segmentation of adipose tissue a threshold-based semi-automatic method was employed using specialized open source software (Slicer, v4.10.2, http://www.slicer.org/) (19). The threshold range was set from −190 to −30 HU (7). Visceral adipose tissue (VAT) was defined as all adipose tissue within the abdominal and pelvic cavity from below the diaphragm to the slice of the upper margin of the pubic symphysis. Subcutaneous adipose tissue (SAT) was defined as all SAT below the slice of the lower margin of Th10 to the slice of the upper margin of the pubic symphysis (*Figure 1*). To ensure consistency of segmentation, five datasets were initially segmented

Table 1 Patient characteristics and scan demographics

Parameter	Value
Age (years)	69.3±12.5
Female	13 (41.9)
Height (cm)	169.5±7.1
Weight (kg)	77.5±15.9
BMI (kg/m^2)	26.9±4.7
100 kV	28 (90.3)
120 kV	2 (6.5)
140 kV	1 (3.2)
Normalized DLP (mGy/cm)	0.96±0.27

Data are mean ± standard deviation or count and (percentage). BMI, body mass index; DLP, dose length product. Normalized DLP is computed as DLP divided by scan length in cm.

for training multiple times. After reliably identifying the chosen landmarks and obtaining very consistent data no intra- or inter-observer agreement was taken. Volume and density were recorded separately for these compartments. Segmentation of SAT and VAT took approximately 20 minutes per scan.

Total adipose tissue (TAT) was calculated as follows:

$$TAT_{density} = VAT_{density} \cdot \frac{VAT_{volume}}{TAT_{volume}} + SAT_{density} \cdot \frac{SAT_{volume}}{TAT_{volume}} \quad [1]$$

$$TAT_{volume} = VAT_{volume} + SAT_{volume} \quad [2]$$

Statistical analysis

Continuous variables are given as mean and standard deviation when symmetrically distributed or as median and interquartile range for skewed distributions; categorical variables are presented as count and percentage.

For intrapatient differences between NES and CES measurements (more precisely, difference CES – NES) a paired *t*-test was applied; for relative differences of NES and CES measurements (i.e., ratio CES/NES) a one-sample *t*-test was used. In contrast to the differences, ratios were log-transformed to guarantee approximately normally distributed variables. All tests were performed at a significance level of 5%. In addition, 95% confidence intervals were calculated for the estimated sample means.

For assessing the relationship between measurements of NES and CES, linear regression analyses were performed. For validation of the regression models, each sample was randomly divided into training and test group at a proportion of 75:25 (ART: 17:6 patients; PVN: 7:3; VEN: 23:8). Linear regression models were derived using only the training data and subsequently validated using the test data. For this purpose, root-mean-square error (RMSE) was calculated for both data sets and compared.

All statistical analyses were performed using R (v3.6.2, R Foundation for Statistical Computing, Vienna, Austria).

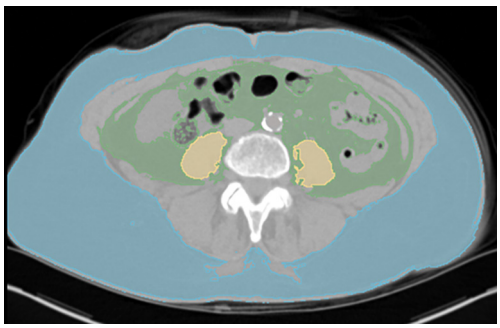

Figure 1 Example of the semi-automatic segmentation of adipose tissue at L4 with thresholds set between –190 and –30 HU. Visceral adipose tissue is marked in green, subcutaneous adipose tissue is marked in blue. The psoas muscles are marked in yellow (not part of this analysis).

Results

Densities of adipose tissue segmented in NES and CES are detailed in *Table 2*. After application of ICM, mean density between NES and CES increased significantly (P<0.001) in all compartments (TAT, VAT and SAT) with the exception of SAT on ART (+0.4±1.5 HU, P=0.19). The changes in density were more pronounced in the visceral compartment (VAT > TAT > SAT) and increased over time after injection of ICM, being more marked in later contrast phases (VEN ≈ PVN > ART).

The volumes of adipose tissue segmented in NES and CES are presented in detail in *Table 3*. Volume of VAT and also of TAT decreased significantly in all CES (P<0.001): VAT in ART: –4.64% (4.29); VAT in PVN: –10.23% (5.77) and VAT in VEN: –9.45% (7.71). The volume of segmented SAT did not change significantly between NES and neither CES [ART: –1.32% (6.88), P=0.37; PVN: –0.53% (7.30), P=0.62; VEN: –2.61% (6.97), P=0.38]. Similarly to density, the changes in volume were more pronounced in later CES

Table 2 Density of segmented adipose tissue in non-enhanced and contrast enhanced scans

Variables	NES (HU)	CES (HU)	Change (HU)	P	95% CI (HU)	R^2	P	Conversion formula	$RMSE_{train}$ (HU)	$RMSE_{test}$ (HU)
NES *vs.* ART (n=23)										
TAT	−89.8±11.9	−89.3±11.1	0.9±1.1	<0.001	[0.4, 1.4]	0.995	<0.001	−0.881+0.999× ART	0.82	1.82
VAT	−84.0±12.1	−83.5±11.3	1.8±1.6	<0.001	[1.1, 2.5]	0.990	<0.001	−1.842+0.998× ART	1.08	2.51
SAT	−93.9±12.8	−93.6±11.8	0.4±1.5	0.19	[−0.2, 1.1]	0.985	<0.001	1.347+1.021× ART	1.48	1.62
NES *vs.* PVN (n=10)										
TAT	−89.8±11.9	−90.7±9.5	3.2±1.7	<0.001	[2.0, 4.3]	0.986	<0.001	−5.626+0.970× PVN	1.40	2.26
VAT	−84.0±12.1	−79.8±10.7	4.4±1.7	<0.001	[3.2, 5.7]	0.982	<0.001	−4.620+1.000× PVN	1.51	2.27
SAT	−93.9±12.8	−97.3±9.1	2.9±1.6	<0.001	[1.8, 4.1]	0.974	<0.001	−5.990+0.968× PVN	1.53	1.85
NES *vs.* VEN (n=31)										
TAT	−89.8±11.9	−86.8±11.4	3.1±2.3	<0.001	[2.2, 3.9]	0.946	<0.001	2.186+1.062× VEN	2.48	2.02
VAT	−84.0±12.1	−80.2±11.1	3.8±3.9	<0.001	[2.4, 5.2]	0.923	<0.001	−2.243+1.028× VEN	3.14	5.57
SAT	−93.9±12.8	−91.1±12.7	2.8±2.2	<0.001	[2.0, 3.6]	0.961	<0.001	−5.015+0.976× VEN	2.39	1.95

Data are mean ± standard deviation. The first P value column (and 95% CI) corresponds to the change between CES and NES while the second P value column corresponds to the difference of the correlation coefficient R from zero. All conversion formulae calculate NES densities in HU. ART, arterial scan; CES, contrast enhanced scan; CI, confidence interval; NES, non-enhanced scan; PVN, portal-venous scan; R^2, coefficient of determination; RMSE, root-mean-square error; SAT, subcutaneous adipose tissue; TAT, total adipose tissue; test, test data; train, training data; VAT, visceral adipose tissue; VEN, venous scan.

(VEN ≈ PVN > ART), but were only significant in the visceral compartment and TAT.

The linear regression models constructed for NES and CES for density and volume (*Tables 2,3*, *Figures 2,3*) show a good fit to the respective data points. However, the goodness of fit of these models increases consistently for volume when considering VAT and SAT separately, shown by smaller RMSE, respectively (*Figure 3*, *Table 3*).

Discussion

The application of ICM changes the results of segmentation of adipose tissue, a key metric for body composition analysis. The effect of ICM on the results of segmentation is influenced by the time elapsed after application and differs between the compartments of the abdomen. If not accounted for, this may lead to falsely low visceral and therefore also total adipose tissue segmented on contrast enhanced CT scans. This may be an important source of bias when trying to compare results to previous studies, which may be adjusted for.

ICM increases the density of adipose tissue segmented on CT. This effect increases with the time elapsed from the application of ICM (arterial < PVN ≈ VEN) and is more pronounced in visceral adipose tissue (VAT) when compared to total (TAT) or subcutaneous adipose tissue (SAT). Furthermore, the application of ICM led to significantly decreased volumes of VAT and therefore also TAT segmented on contrast enhanced CT compared to non-enhanced CT. The effect of ICM on the segmented amount of SAT was smaller and not statistically significant; however, this is most likely attributed to the limited number of scans available for analysis. Similarly to density, the effect of ICM on segmented volume of adipose tissue was least pronounced in arterial and most pronounced in later scans (PVN, venous).

It is well known that scan parameters (kV; mAs) have a direct effect on CT-density of tissues and therefore may also influence segmentations of adipose tissue (14,20). As scan parameters were kept identical between scans, we could exclude this bias from our analysis. Furthermore, a fixed volume of ICM was applied to all patients, regardless of body weight or body mass index. Finally, we decided in favor of 3D-segmentation of the entire abdominal cavity

Table 3 Volume of segmented adipose tissue in non-enhanced and contrast enhanced scans

Variables	NES (dm^3)	CES (dm^3)	Change (%)	P	95% CI (%)	R^2	P	Conversion formula	$RMSE_{train}$ (dm^3)	$RMSE_{test}$ (dm^3)
NES *vs.* ART (n=23)										
TAT	10.68±4.84	10.85±5.13	−3.71 (5.72)	<0.001	[−4.64, −1.45]	0.994	<0.001	0.426+0.979*ART	0.41	0.52
VAT	4.82±2.23	4.85±2.22	−4.64 (4.29)	<0.001	[−6.80, −3.73]	0.995	<0.001	0.154+1.012*ART	0.18	0.14
SAT	5.86±3.31	6±3.61	−1.32 (6.88)	0.37	[−3.63, 1.44]	0.986	<0.001	0.176+0.983*ART	0.36	0.45
NES *vs.* PVN (n=10)										
TAT	10.68±4.84	10.92±4.97	−3.23 (7.58)	0.029	[−10.40, −0.77]	0.994	<0.001	1.688+0.890*PVN	0.35	0.77
VAT	4.82±2.23	4.26±2.14	−10.23 (5.77)	0.002	[−17.20, −5.63]	0.989	<0.001	0.228+1.066*PVN	0.22	0.28
SAT	5.86±3.31	6.66±3.27	−0.53 (7.30)	0.62	[−4.86, 3.19]	0.987	<0.001	0.937+0.862*PVN	0.32	0.55
NES *vs.* VEN (n=31)										
TAT	10.68±4.84	10.25±4.85	−4.72 (8.72)	<0.001	[−8.15, −3.09]	0.985	<0.001	0.294+1.024*VEN	0.59	0.84
VAT	4.82±2.23	4.46±2.35	−9.45 (7.71)	<0.001	[−15.20, −7.63]	0.988	<0.001	0.394+1.018*VEN	0.23	0.81
SAT	5.86±3.31	5.8±3.26	−2.61 (6.97)	0.38	[−4.48, 1.81]	0.966	<0.001	0.232+0.974*VEN	0.54	0.64

Data are mean ± standard deviation in dm^3 or median in percent and (interquartile range in percentage points). The first P value column (and 95% CI) corresponds to the relative change between CES and NES while the second P value column corresponds to the difference of the correlation coefficient R from zero. All conversion formulae calculate NES volumes in dm^3. ART, arterial scan; CES, contrast enhanced scan; CI, confidence interval; NES, non-enhanced scan; PVN, portal-venous scan; R^2, coefficient of determination; RMSE, root-mean-square error; SAT, subcutaneous adipose tissue; TAT, total adipose tissue; test, test data; train, training data; VAT, visceral adipose tissue; VEN, venous scan.

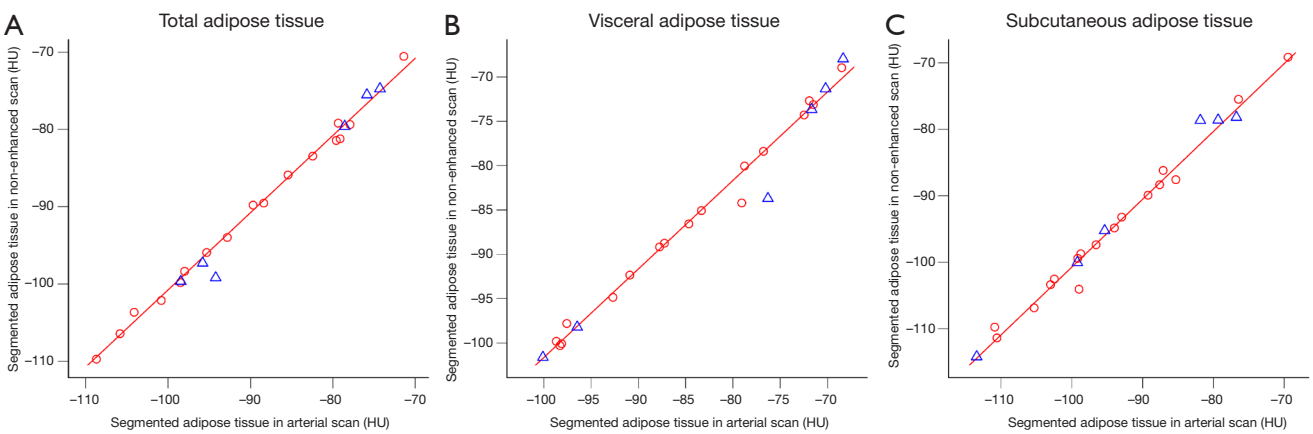

Figure 2 Linear regression models for density of segmented adipose tissue (solid red line) fitted to randomly selected training data (red circles) for the abdominal compartments (A,B,C). Test data points are shown as blue triangles. All models achieve very good fit with similarly small root-mean-square errors for both training and test data (for details see *Table 2*).

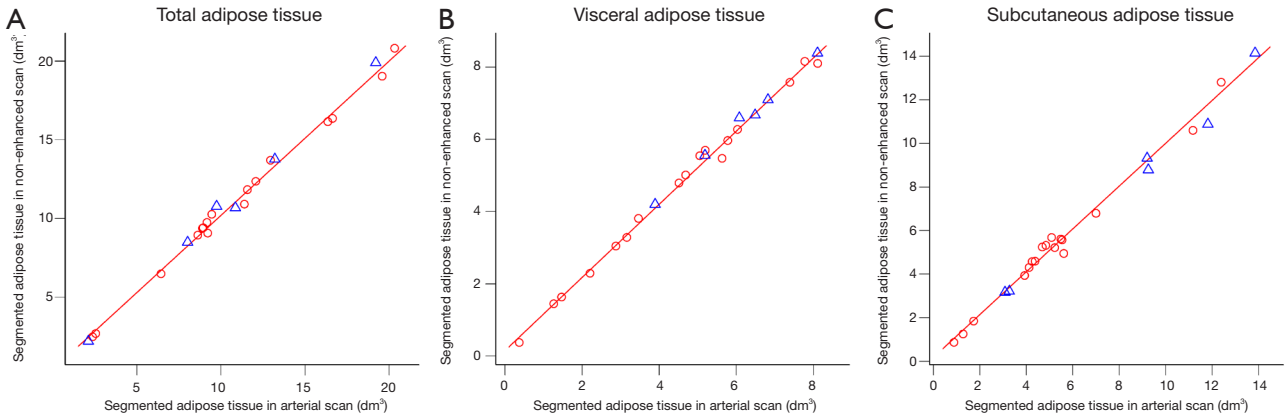

Figure 3 Linear regression models for volume of segmented adipose tissue (solid red line) fitted to randomly selected training data (red circles) for the abdominal compartments (A,B,C). Test data points are shown as blue triangles. All models achieve very good fit with small root-mean-square errors for both training and test data. Note the different scales and slightly higher deviation of data points from the regression model for total abdominal adipose tissue (A) compared to the visceral and subcutaneous compartments (B,C) and ultimately smaller root-mean-square errors when considering the visceral and subcutaneous compartment separately (see also *Table 3*).

including several hundred slices per scan. This helped to characterize the influence of ICM on segmentation more robustly through the contrast phases and minimize noise, rather than introducing additional bias, which otherwise would have made necessary a much larger number of examinations to be assessed.

Our findings of decreased TAT in PVN (median: −3.23%; mean: −5.72%) are in line with the previously observed changes in area in the present literature (reported mean PVN: −6.5%) (14). The results of another study are somewhat lower (mean ART: −2.05%, PVN: −2.44%); however, these results are more difficult to interpret as the area was converted to total body fat and the important potentially confounding factors of scan settings (mAs and kV) between the scans were not reported (16). The only other publication on this topic did not provide a delay after injection of ICM and dosed the amount according to bodyweight, and finds a positive correlation of change (smaller area of segmented VAT) with body weight (15). As this study dosed the amount of ICM according to body weight and distribution of ICM takes place in the extracellular space, which in turn is more closely related to lean body mass rather than body weight, we believe this observation to be biased.

To our knowledge, we are the first to describe the changes of segmented adipose tissue after injection of ICM separately in both visceral and subcutaneous compartments for multiple contrast phases. We present clear evidence that the observed effects increase with the delay after injection and vary in degree between VAT and SAT and therefore ultimately also in TAT.

We attribute the differing degree of changes in density and ultimately volume changes of segmented VAT and SAT after application of ICM to differing anatomical conditions and physiological roles within the compartments, which also may have to do with a different developmental origin (21,22). The adipose tissue within the visceral compartment is closely intertwined with organs, large and medium size vessels and actively participates in metabolism. Furthermore, it is believed to have endocrine function (11,23). In contrast, the subcutaneous compartment is structured much more homogeneously with only very small blood vessels, relatively clear borders and much fewer tissue interfaces. Therefore, it seems quite evident that ICM is not only carried to the VAT more promptly, but that the extracellular spaces intertwined with it are much larger than those of SAT. This leads to an elevation of density and/or misclassification of voxels in CES, which otherwise with the given threshold in NES would have been classified as adipose tissue. This is most likely a result of partial volume effect. The intensity of this seems to correlate with the delay after application of ICM, being less pronounced in ART with the contrast medium being mainly in the arteries, and being more pronounced in later scans when the contrast medium is present in both arteries and veins.

One may obtain values of segmented adipose tissue

in NES from CES by either adjusting the upper limit of the threshold range (15) or by means of conversion formulae. Since conversion formulae are much easier to apply retrospectively, rather than individually adjusting the threshold range, we deem this approach more feasible. As the alterations of density and volume of segmented adipose tissue introduced by ICM are fairly predictable, contrast enhanced CT allows for the estimation of density and volume of adipose tissue measurable in non-enhanced CT by means of conversion formulae derived from linear regression analyses with remarkable precision. The achieved small RMSE speaks for the robustness of this approach despite the relatively moderate number of scans (*Tables 2,3*). The estimation becomes particularly precise for volumes when considering the visceral and subcutaneous compartments separately. With the help of these conversion formulae, results obtained from CES may be converted to those of NES and compared to those of previous studies using NES.

This conversion allows for the comparison of the results of body composition analysis obtained from CES to results using either NES or different CES within the same individual or even previous studies. This may aid in a more valid assessment of frailty or risk stratification.

Limitations

Our study is retrospective in design and comprises only a moderate number of patients. Moreover, not all contrast phases were available for each patient. This made it particularly difficult to precisely characterize the influence of ICM on PVN with the fewest scans included and similar changes compared to VEN. Furthermore, volume differences for SAT were smaller and did not reach statistical significance, also most likely attributable to the moderate sample size. However, as mainly intraindividual differences were assessed at a single point in time, identical scan settings were used and the entire abdominal cavity with several hundred slices per patient were segmented, the sample size was sufficient for characterizing the effect of ICM on segmentation of adipose tissue and for calculating and validating conversion formulae.

No selection or exclusion of potentially interfering medical conditions altering circulation time (e.g., heart failure, sepsis with tachycardia) or extracellular volume (e.g., oncological illness or sepsis) took place. Even though mainly intraindividual differences were observed and the direction and magnitude of change after application of ICM were relatively constant between individuals, the extent of change may still have been influenced by these conditions. Therefore, caution is necessary when applying our findings to other patient cohorts or healthy volunteers.

Conclusions

The density change of adipose tissue after injection of ICM is evident in all compartments, but varies substantially in degree between the visceral and subcutaneous compartment (visceral > total > subcutaneous adipose tissue) and may influence volume segmentation.

As the effect of contrast medium on density and segmented volume is fairly constant in a given contrast phase and compartment, density and particularly volume of adipose tissue may be accurately calculated from the segmentation of contrast enhanced CT examinations.

Acknowledgments

The authors thank Werner Daßler for his kind support in language editing. We acknowledge the position of Robin F. Gohmann to have been equally funded by Leipzig University and Leipzig Heart Center. We acknowledge support from Leipzig University for Open Access Publishing.
Funding: None.

Footnote

Conflicts of Interest: All authors have completed the ICMJE uniform disclosure form (available at http://dx.doi.org/10.21037/qims-20-907). The authors have no conflicts of interest to declare.

Ethical Statement: The study was conducted in compliance with the Declaration of Helsinki (Medical Association 2013). The institutional ethics committee of Leipzig University approved the study (reference number: 337/19-ek) and written informed consent was waived, because the study was retrospective in design.

References

1. Foldyna B, Troschel FM, Addison D, Fintelmann FJ, Elmariah S, Furman D, Eslami P, Ghoshhajra B, Lu MT, Murthy VL, Hoffmann U, Shah R. Computed tomography-based fat and muscle characteristics are associated with mortality after transcatheter aortic valve replacement. J Cardiovasc Comput Tomogr 2018;12:223-8.
2. Kalafateli M, Mantzoukis K, Choi Yau Y, Mohammad AO, Arora S, Rodrigues S, de Vos M, Papadimitriou K, Thorburn D, O'Beirne J, Patch D, Pinzani M, Morgan MY, Agarwal B, Yu D, Burroughs AK, Tsochatzis EA. Malnutrition and sarcopenia predict post-liver transplantation outcomes independently of the Model for End-stage Liver Disease score. J Cachexia Sarcopenia Muscle 2017;8:113-21.
3. Popinat G, Cousse S, Goldfarb L, Becker S, Gardin I, Salaün M, Thureau S, Vera P, Guisier F, Decazes P. Subcutaneous Fat Mass measured on multislice computed tomography of pretreatment PET/CT is a prognostic factor of stage IV non-small cell lung cancer treated by nivolumab. Oncoimmunology 2019;8:e1580128.
4. Prado CM, Lieffers JR, McCargar LJ, Reiman T, Sawyer MB, Martin L, Baracos VE. Prevalence and clinical implications of sarcopenic obesity in patients with solid tumours of the respiratory and gastrointestinal tracts: a population-based study. Lancet Oncol 2008;9:629-35.
5. Shuster A, Patlas M, Pinthus JH, Mourtzakis M. The clinical importance of visceral adiposity: a critical review of methods for visceral adipose tissue analysis. Br J Radiol 2012;85:1-10.
6. Doyle SL, Bennett AM, Donohoe CL, Mongan AM, Howard JM, Lithander FE, Pidgeon GP, Reynolds JV, Lysaght J. Establishing computed tomography-defined visceral fat area thresholds for use in obesity-related cancer research. Nutr Res 2013;33:171-9.
7. Kvist H, Sjöström L, Tylén U. Adipose tissue volume determinations in women by computed tomography: technical considerations. Int J Obes 1986;10:53-67.
8. Borkan GA, Gerzof SG, Robbins AH, Hults DE, Silbert CK, Silbert JE. Assessment of abdominal fat content by computed tomography. Am J Clin Nutr 1982;36:172-7.
9. Mitsiopoulos N, Baumgartner RN, Heymsfield SB, Lyons W, Gallagher D, Ross R. Cadaver validation of skeletal muscle measurement by magnetic resonance imaging and computerized tomography. J Appl Physiol 1998;85:115-22.
10. Sjöström L, Kvist H, Cederblad A, Tylén U. Determination of total adipose tissue and body fat in women by computed tomography, 40K, and tritium. Am J Physiol 1986;250:E736-45.
11. Maurovich-Horvat P, Massaro J, Fox CS, Moselewski F, O'Donnell CJ, Hoffmann U. Comparison of anthropometric, area- and volume-based assessment of abdominal subcutaneous and visceral adipose tissue volumes using multi-detector computed tomography. Int J Obes (Lond) 2007;31:500-6.
12. Mourtzakis M, Prado CMM, Lieffers JR, Reiman T, McCargar LJ, Baracos VE. A practical and precise approach to quantification of body composition in cancer patients using computed tomography images acquired during routine care. Appl Physiol Nutr Metab 2008;33:997-1006.
13. Irlbeck T, Massaro JM, Bamberg F, O'Donnell CJ, Hoffmann U, Fox CS. Association between single-slice measurements of visceral and abdominal subcutaneous adipose tissue with volumetric measurements: the Framingham Heart Study. Int J Obes (Lond) 2010;34:781-7.
14. Morsbach F, Zhang YH, Martin L, Lindqvist C, Brismar T. Body composition evaluation with computed tomography: Contrast media and slice thickness cause methodological errors. Nutrition 2019;59:50-5.
15. Vehmas T, Kairemo KJ, Taavitsainen MJ. Measuring visceral adipose tissue content from contrast enhanced computed tomography. Int J Obes Relat Metab Disord 1996;20:570-3.
16. Rollins KE, Javanmard-Emamghissi H, Awwad A, Macdonald IA, Fearon KCH, Lobo DN. Body composition measurement using computed tomography: Does the phase of the scan matter? Nutrition 2017;41:37-44.
17. Madico C, Herpe G, Vesselle G, Boucebci S, Tougeron D, Sylvain C, Ingrand P, Tasu JP. Intra peritoneal abdominal fat area measured from computed tomography is an independent factor of severe acute pancreatitis. Diagn Interv Imaging 2019;100:421-6.
18. Okuno T, Koseki K, Nakanishi T, Ninomiya K, Tomii D, Tanaka T, Sato Y, Osanai A, Sato K, Koike H, Yahagi K, Kishi S, Komiyama K, Aoki J, Yokozuka M, Miura S, Tanabe K. Prognostic Impact of Computed Tomography-Derived Abdominal Fat Area on Transcatheter Aortic Valve Implantation. Circ J 2018;82:3082-9.

19. Fedorov A, Beichel R, Kalpathy-Cramer J, Finet J, Fillion-Robin JC, Pujol S, Bauer C, Jennings D, Fennessy F, Sonka M, Buatti J, Aylward S, Miller JV, Pieper S, Kikinis R. 3D Slicer as an image computing platform for the Quantitative Imaging Network. Magn Reson Imaging 2012;30:1323-41.
20. Morsbach F, Zhang YH, Nowik P, Martin L, Lindqvist C, Svensson A, Brismar TB. Influence of tube potential on CT body composition analysis. Nutrition 2018;53:9-13.
21. Chau YY, Bandiera R, Serrels A, Martínez-Estrada OM, Qing W, Lee M, Slight J, Thornburn A, Berry R, McHaffie S, Stimson RH, Walker BR, Chapuli RM, Schedl A, Hastie N. Visceral and subcutaneous fat have different origins and evidence supports a mesothelial source. Nat Cell Biol 2014;16:367-75.
22. Hwang I, Kim JB. Two Faces of White Adipose Tissue with Heterogeneous Adipogenic Progenitors. Diabetes Metab J 2019;43:752-62.
23. Misra M, Bredella MA, Tsai P, Mendes N, Miller KK, Klibanski A. Lower growth hormone and higher cortisol are associated with greater visceral adiposity, intramyocellular lipids, and insulin resistance in overweight girls. Am J Physiol Endocrinol Metab 2008;295:E385-92.

Cite this article as: Gohmann RF, Gottschling S, Seitz P, Temiz B, Krieghoff C, Lücke C, Horn M, Gutberlet M. 3D-segmentation and characterization of visceral and abdominal subcutaneous adipose tissue on CT: influence of contrast medium and contrast phase. Quant Imaging Med Surg 2021;11(2):697-705. doi: 10.21037/qims-20-907

